Constraining the hidden-charm pentaquark predictions and discriminating the $P_c(4440)$ and $P_c(4457)$ spins through the effective range expansion

Fang-Zheng Peng,[1] Li-Sheng Geng,[2,1,3,4,*] and Ju-Jun Xie[1,5,6,†]

[1]*Southern Center for Nuclear-Science Theory (SCNT), Institute of Modern Physics, Chinese Academy of Sciences, Huizhou 516000, China*
[2]*School of Physics, Beihang University, Beijing 102206, China*
[3]*Peng Huanwu Collaborative Center for Research and Education, Beihang University, Beijing 100191, China*
[4]*Beijing Key Laboratory of Advanced Nuclear Materials and Physics, Beihang University, Beijing 102206, China*
[5]*Heavy Ion Science and Technology Key Laboratory, Institute of Modern Physics, Chinese Academy of Sciences, Lanzhou 730000, China*
[6]*School of Nuclear Sciences and Technology, University of Chinese Academy of Sciences, Beijing 101408, China*

(Received 22 November 2024; accepted 6 March 2025; published 25 March 2025)

The Weinberg compositeness criterion dictates that a pure shallow bound state is characterized by a large scattering length $a_0 \gg \mathcal{O}(1/\beta)$ and a positive effective range r_0 that naturally scales to the size of $\mathcal{O}(1/\beta)$, where $1/\beta$ signifies the interaction range. In constructing the contact-range effective field theory (EFT) up to the next-to-leading order to describe the pentaquarks $P_c(4312)$, $P_c(4440)$, and $P_c(4457)$ observed by the LHCb collaboration in 2019, we match the effective range r_0 at single-channel situation for these pentaquarks with the low-energy couplings within the EFT framework. Three different schemes are used to connect the couplings with the effective range. We find positive effective ranges r_0 of the natural size of $\mathcal{O}(1/\beta)$ for the spin configurations $J^P = \frac{3}{2}^-$ for $P_c(4440)$ and $J^P = \frac{1}{2}^-$ for $P_c(4457)$ within the molecular $\bar{D}^*\Sigma_c$ description. Additionally, predictions from the power counting for low-energy couplings or Wilsonian coefficients suggest that, under heavy quark spin symmetry, the broad $P_c(4380)$ resonance, discovered by the LHCb collaboration in 2015, when considered as part of the single-channel $\bar{D}^{(*)}\Sigma_c^{(*)}$ molecular system alongside $P_c(4312)$, $P_c(4440)$, and $P_c(4457)$, has a mass of approximately 4376 MeV.

DOI: 10.1103/PhysRevD.111.054029

I. INTRODUCTION

The theoretical and experimental investigation of multiquark exotic hadrons, which transcend the conventional quark model description, has consistently triggered substantial interest due to their potential implications for our understanding of nonperturbative quantum chromodynamics [1–5]. In 2015, two hidden-charm pentaquark states, $P_c(4380)$ and $P_c(4450)$, were first discovered by the LHCb experiment [6]. Subsequent observations revealed that the $P_c(4450)$ splits into two narrow peaks, namely, $P_c(4440)$ and $P_c(4457)$, and a new $P_c(4312)$ state was also identified. However, the broad $P_c(4380)$ does not appear as a clear signal in the $J/\psi p$ mass spectrum [7]. These three pentaquarks, $P_c(4312)$ (P_{c1}), $P_c(4440)$ (P_{c2}), and $P_c(4457)$ (P_{c3}), have sparked lively discussions regarding their nature [8–18]. Their masses and widths are

$$m(P_{c1}) = 4311.9 \pm 0.7^{+6.8}_{-0.6}\ \text{MeV},$$
$$\Gamma(P_{c1}) = 9.8 \pm 2.7^{+3.7}_{-4.5}\ \text{MeV}, \quad (1)$$

$$m(P_{c2}) = 4440.3 \pm 1.3^{+4.1}_{-4.7}\ \text{MeV},$$
$$\Gamma(P_{c2}) = 20.6 \pm 4.9^{+8.7}_{-10.1}\ \text{MeV}, \quad (2)$$

$$m(P_{c3}) = 4457.3 \pm 0.6^{+4.1}_{-1.7}\ \text{MeV},$$
$$\Gamma(P_{c3}) = 6.4 \pm 2.0^{+5.7}_{-1.9}\ \text{MeV}. \quad (3)$$

Since their masses are close to the $\bar{D}\Sigma_c$ and $\bar{D}^*\Sigma_c$ thresholds, it is natural to consider them as molecules of charmed mesons and baryons [19–33]. Besides, there exist

*Contact author: lisheng.geng@buaa.edu.cn
†Contact author: xiejujun@impcas.ac.cn

other explanations for these pentaquarks, e.g., compact five quark states and hadrocharmonia [34–39].

Within the molecular picture, heavy quark spin symmetry (HQSS) implies other four pentaquarks formed by $\bar{D}\Sigma_c^*$ and $\bar{D}^*\Sigma_c^*$ [40,41], which together with the above three pentaquarks already identified by the LHCb collaboration, constitute a multiplet of seven pentaquark states. Furthermore, within this hadronic molecular framework, the mass spectrum alone derived from the effective field theory or phenomenology does not allow for a definitive determination of the $P_c(4440)$ and $P_c(4457)$ spins, which can be either $J^P = \frac{1}{2}^-$ or $\frac{3}{2}^-$. Many studies have addressed this spin issue [42–46]. To determine the P_{c2} and P_{c3} spins under the two-body hadronic molecular $\bar{D}^*\Sigma_c$ description, it is helpful to reconsider the nature of being "molecule" or "composite." For a given few-body system on a low energy scale, the Weinberg compositeness criterion could judge whether this system is "composite" or more like "elementary." The Weinberg compositeness criterion was originally proposed for studying the deuteron to discriminate between the elementary particle $|d\rangle$ and the composite molecular state $|np\rangle$, and this criterion has been extended to exotic hadronic states. A multiquark state $|\Phi\rangle$ can contain two components, a compact one $|\phi\rangle$ and a two-body molecular part $|h_1h_2(\mathbf{k})\rangle$

$$|\Phi\rangle = \sqrt{Z}|\phi\rangle + \int \frac{d^3\mathbf{k}}{(2\pi)^3}\lambda(\mathbf{k})|h_1h_2(\mathbf{k})\rangle, \tag{4}$$

with h_i (i = 1, 2) representing the hadrons in the molecule picture. $Z = |\langle\Phi|\phi\rangle|^2$ and $1 - Z = \int \frac{d^3\mathbf{k}}{(2\pi)^3}|\lambda(\mathbf{k})|^2$ indicate the probability of the compact and molecular parts within the given system, respectively.

For an s-wave loosely bound state, the Weinberg compositeness criterion connects the renormalization factor Z to the scattering length a and effective range r. For a pure molecular state, the derivation above yields the condition $Z = 0$, which implies that the scattering length a should be *unnaturally* large, namely, $a \gg 1/\Lambda$ with Λ the hard energy scale of the molecular system, while the effective range r is positive and of the order of the range $\mathcal{R}$ of the potential responsible for binding the molecular state.

This study aims to investigate the effective ranges of the $P_c(4312)$, $P_c(4440)$, and $P_c(4457)$ states within the molecular picture and the contact effective field theory framework. We will consider two alternative scenarios with distinct $\bar{D}^*\Sigma_c$ spin configurations for $P_c(4440)$ and $P_c(4457)$ to calculate the effective range. By evaluating which scenario yields a *unnaturally* large scattering length a and a positive effective range r comparable to the interaction range $\mathcal{R}$—consistent with the molecular hypothesis with $Z = 0$—we aim to determine the spins of $P_c(4440)$ and $P_c(4457)$. Besides, the existence of other predicted P_c molecular states under HQSS will be examined, which is important for future experiments and understanding the pentaquarks' nature.

This article is structured as follows. In Sec. II, we derive the effective range and scattering length for pure molecules by revisiting the Weinberg compositeness. In Sec. III, we construct the next-to-leading order contact field theory to describe the P_c states within the molecular picture. The corresponding power counting is introduced in Sec. IV. Three matching schemes to relate the effective range to low-energy couplings are proposed in Sec. V. The numerical results are presented in Sec. VI. Finally, Sec. VII provides our conclusions and discussions.

II. EFFECTIVE RANGE EXPANSION AND THE WEINBERG COMPOSITENESS OF BOUND STATES

Considering the P_c states as two-body bound system of $\bar{D}^{(*)}\Sigma_c^{(*)}$, the effective range expansion at low momenta p yields [47,48]

$$p^{2l+1}\cot\delta_l = -\frac{1}{a_l} + \frac{1}{2}r_l p^2 + \cdots, \tag{5}$$

where $l = 1, 2, 3, \ldots$ represent the different partial waves, δ_l is the phase shift, a_l and r_l are respectively the scattering length and effective range. The s-wave amplitude in a low-energy scattering process can then be written

$$\mathcal{T} = \frac{2\pi}{\mu}\frac{1}{p\cot\delta_0 - ip} = \frac{2\pi}{\mu}\frac{1}{-\frac{1}{a_0} + \frac{1}{2}r_0p^2 + \cdots}, \tag{6}$$

with μ denoting the reduced mass of the two-body bound system.

The binding momentum for the $\bar{D}^{(*)}\Sigma_c^{(*)}$ molecules is $\gamma = \sqrt{2\mu E_B}$, where $E_B > 0$ is the binding energy. For loosely bound states, $\gamma \ll \beta$, where β is the hard energy scale of the two-body system, usually represented by the mass of the exchanged meson $m_{\rm ex}$. The compositeness $1 - Z$ under the nonrelativistic situation could be written as the following [49,50]

$$\begin{aligned} 1 - Z &= \int \frac{d^3\mathbf{k}}{(2\pi)^3}\frac{\langle h_1h_2(\mathbf{k})|V|\Phi\rangle}{\left(E_B + \frac{\mathbf{k}^2}{2\mu}\right)^2}\left(1 + \mathcal{O}\left(\frac{\mathbf{k}^2}{\beta^2}\right)\right) \\ &= \frac{\mu^2 g^2}{2\pi\gamma}\left(1 + \mathcal{O}\left(\frac{\gamma}{\beta}\right)\right), \end{aligned} \tag{7}$$

where V is the interaction between the state $|\Phi\rangle$ and the hadron pair, and the constant $g \simeq \langle h_1h_2(\mathbf{k})|V|\Phi\rangle$ introduced here is the coupling between the molecular system and the given state. Through the dispersion relation of $\mathcal{T}$, this coupling g can be connected to the scattering

amplitude. Comparing with $\mathcal{T}$ in Eq. (6), the Weinberg compositeness could be obtained as [51,52]

$$a_0 = 2\frac{(1-Z)}{\gamma(2-Z)} + \mathcal{O}\left(\frac{1}{m_{\rm ex}}\right), \tag{8}$$

$$r_0 = -\frac{Z}{\gamma(1-Z)} + \mathcal{O}\left(\frac{1}{m_{\rm ex}}\right). \tag{9}$$

We note that the compositeness $1-Z$ is very sensitive to a_0 and r_0, because the compositeness $1-Z = \sqrt{a_0/(a_0-2r_0)}$ becomes singular at $r_0 = a_0/2$. On the other hand, the effective range r_0 and scattering length a_0 of the deuteron can be well described by assuming $Z=0$ [50]. In this work, we assume that the above relations hold. More extensive studies on the limitations and extensions of the Weinberg compositeness criterion, including scenarios involving virtual states, resonant states and coupled-channel scenario, can be found in Refs. [52–59].

According to the above relations among a_0, r_0, and the compositeness $1-Z$, for a pure molecular system with $Z=0$, the effective range r_0 is positive [60–62], with a value of the order of the interaction range of $\mathcal{O}(1/m_{\rm ex}) \sim \mathcal{R}$. Conversely, for a compact state with $Z=1$, r_0 is negative. Additionally, under the low-energy situation of $\gamma \ll m_{\rm ex}$, assuming $Z=0$ for a molecule leads to an *unnaturally* large scattering length $a_0 \sim 1/\gamma \gg \mathcal{R}$. This is consistent with the characteristics of shallow bound states, as the scattering length a_0 could be interpreted as the node of the wave function $\phi(x)$ at low energy k [63]

$$\phi(x) \sim \sin(kx+\delta_0) \sim 1 - \frac{x}{a_0}. \tag{10}$$

The emergence of a shallow bound state will alter a_0 from infinity to an *unnaturally* large magnitude.

Therefore, the molecular hypothesis for the pentaquark states as $\bar{D}^{(*)}\Sigma_c^{(*)}$ bound states imply positive natural effective ranges $r_0 \sim \mathcal{R}$ and unnaturally large scattering lengths of $a_0 \gg \mathcal{R}$ for the $\bar{D}^{(*)}\Sigma_c^{(*)}$ interactions. However, it should be noted here that the above conclusion is for *bound states* since the application of the Weinberg compositeness criterion to virtual or resonance states is different [54,56,57,64,65]. In addition, the assumption of *pure molecule states* is necessary for obtaining a positive effective range r_0. This is related to the uncertainties from $\mathcal{O}(1/m_{\rm ex})$ and can be understood as follows. Taking, as an example, the requirement of $r_0 > 0$ in Eq. (9), we have

$$\frac{1}{m_{\rm ex}} < \frac{1-Z}{Z}\gamma. \tag{11}$$

For the P_c states studied here, one can assign $m_{\rm ex}$ a value of ∼500 MeV, assuming that the short-range interactions are mediated by the scalar meson of σ and vector mesons of ρ and ω. On the other hand, γ is taken as about 100 MeV [66–68]. As a result, a compact component of $Z \geq 0.2$ will invalidate the relation of Eq. (11) and thus the conclusion of $r_0 > 0$ for bound molecular states. Consequently, the premise of pure molecular states or a negligible fraction of compact components for the P_c states is essential for the above conclusions.

III. MOLECULAR DESCRIPTIONS OF P_c STATES WITH CONTACT EFFECTIVE FIELD THEORY UP TO NEXT-TO LEADING ORDER

The $P_c(4312)$, $P_c(4440)$, and $P_c(4457)$ states can be described as nonrelativistic $\bar{D}^{(*)}\Sigma_c$ bound states in the contact effective field theory [27,40,69,70]. Under HQSS, the LO meson-baryon potential can be expressed with two low-energy couplings

$$V = C_a + C_b(\vec{\sigma}_{1L}\cdot\vec{S}_{2L}), \tag{12}$$

where $\vec{\sigma}_{1L}$ and $\vec{S}_{2L}$ represent the spins of the light degrees of freedom within the charmed mesons and baryons, respectively. According to HQSS, the spins of heavy c quarks do not influence the interactions between the $\bar{D}^{(*)}$ mesons and $\Sigma_c^{(*)}$ baryons. Here, it should be noted that our analysis assumes a single-channel of $\bar{D}^{(*)}\Sigma_c$ configuration, where we study with the isospin-symmetric limit and use the isospin-averaged masses of $\bar{D}^{(*)}$ and Σ_c as listed in the Particle Data Group (PDG) [71]. The above contact potential yields the following potentials for the $\bar{D}\Sigma_c$ and $\bar{D}^*\Sigma_c$ systems

$$V\left(\bar{D}\Sigma_c; J^P = \frac{1}{2}^-\right) = C_a, \tag{13}$$

$$V\left(\bar{D}^*\Sigma_c; J^P = \frac{1}{2}^-\right) = C_a - \frac{4}{3}C_b, \tag{14}$$

$$V\left(\bar{D}^*\Sigma_c; J^P = \frac{3}{2}^-\right) = C_a + \frac{2}{3}C_b. \tag{15}$$

However, the spin classification of $\bar{D}^*\Sigma_c$ for $P_c(4440)$ and $P_c(4457)$ remains undetermined from the mass spectra studies with the above LO potential. $P_c(4440)$ and $P_c(4457)$ can either have $J^P = \frac{1}{2}^-$ or $\frac{3}{2}^-$. Both scenarios predict a $\bar{D}\Sigma_c$ bound state, corresponding to $P_c(4312)$, of a similar mass within the experimental uncertainty.

Since the effective range r_0 should be positive and of natural size for pure s-wave bound molecular states, it is useful to calculate r_0 from the contact range EFT to help determine which spin scenario for $P_c(4440)$ and $P_c(4457)$ is preferred. In the scenario where the scattering length $a_0 \sim 1/p \gg \mathcal{R}$ is unnaturally large, to generate the effective range r_0, one needs to construct the contact potential at

least up to the next-to-leading order (NLO) of $\mathcal{O}(p^2)$. This can be easily verified by expanding the amplitude of Eq. (6) [72,73].

In the nonrelativistic effective field theory, the contact interactions between two hadrons are described by the following effective Lagrangian [47,74]

$$\mathcal{L} = \psi^\dagger\left(i\partial_t + \frac{\nabla^2}{2m}\right)\psi + C_0\psi^\dagger\psi\psi^\dagger\psi + C_2[(\psi^\dagger\psi^\dagger)(\psi\overleftrightarrow{\nabla}^2\psi) + \text{H.c.}] + \cdots. \quad (16)$$

From the above Lagrangian, the contact potential V in the center-of-mass system (CMS) can be derived as [75–78]

$$\begin{aligned} V = {} & C_0 + C_2^1 q^2 + C_2^2 k^2 + (C_2^3 q^2 + C_2^4 k^2)\vec{\sigma}_{1L}\cdot\vec{S}_{2L} \\ & + \frac{i}{2}C_2^5(\vec{\sigma}_{1L} + \vec{S}_{2L})\cdot(q\times k) + C_2^6(q\cdot\vec{\sigma}_{1L})(q\cdot\vec{S}_{2L}) \\ & + C_2^7(k\cdot\vec{\sigma}_{1L})(k\cdot\vec{S}_{2L}) + \frac{i}{2}C_2^8(\vec{\sigma}_{1L} - \vec{S}_{2L})\cdot(q\times k) \\ & + \cdots, \end{aligned} \quad (17)$$

where $\vec{p}$ and $\vec{p}'$ are the initial and final center-of-mass momenta, C_0, C_2^i $(i = 1, \ldots, 8)$ are the low-energy couplings, also known as Wilson coefficients in effective field theory, and $q = \vec{p}' - \vec{p}$, $k = (\vec{p}' + \vec{p})/2$ are defined as the transferred and average momenta.

Performing the standard partial-wave projection, the above NLO contact potential can be respectively reduced to the following forms with four low-energy couplings for the s-wave states of ${}^2S_{\frac{1}{2}}$ $\bar{D}\Sigma_c$, ${}^2S_{\frac{1}{2}}$ $\bar{D}^*\Sigma_c$, and ${}^4S_{\frac{3}{2}}$ $\bar{D}^*\Sigma_c$

$$V_1 = C_a + \frac{1}{2}D_a(\vec{p}^2 + \vec{p}'^2) \quad (18)$$

$$V_2 = C_a - \frac{4}{3}C_b + \frac{1}{2}(D_a - D_b)(\vec{p}^2 + \vec{p}'^2) \quad (19)$$

$$V_3 = C_a + \frac{2}{3}C_b + \frac{1}{2}\left(D_a + \frac{D_b}{2}\right)(\vec{p}^2 + \vec{p}'^2). \quad (20)$$

The Lippmann-Schwinger equation of $\mathcal{T} = V + VG\mathcal{T}$ can be greatly simplified in the contact effective field theory. Introducing a Gaussian regulator of the form $e^{-\frac{2q^2}{\Lambda^2}}$ with Λ the momentum cutoff and adopting the on-shell approximation, the scattering amplitude $\mathcal{T}$ becomes

$$\begin{aligned} \mathcal{T} &= V[1 + VG(q,\Lambda) + (VG(q,\Lambda))^2 + \cdots] \\ &= \frac{V}{1 - VG(q,\Lambda)}, \end{aligned} \quad (21)$$

where the propagator G is

$$G(E_B,\Lambda) = \frac{\mu}{\pi^2}\int_0^{+\infty} dq\,\frac{q^2}{2\mu E_B + q^2}e^{-\frac{2q^2}{\Lambda^2}}. \quad (22)$$

Here, μ is the reduced mass of the $\bar{D}^{(*)}\Sigma_c$ system and $E_B > 0$ is the binding energy.

In the unnatural scenario where the scattering length a_0 is large, satisfying $a_0 \sim \frac{1}{p} \gg \frac{1}{\Lambda}$ [corresponding precisely to our case with $Z = 0$ in Eq. (8)], the amplitude $\mathcal{T}$ can be expanded in powers of $\frac{p}{\Lambda}$ rather than p. This expansion is permissible for large a_0 situation, because p is not small compared to $\frac{1}{a_0}$, thereby leading to [47,72,73]

$$\mathcal{T} = -\frac{2\pi}{\mu}\frac{1}{\frac{1}{a_0} + ip}\left[1 + \frac{r_0}{2\left(\frac{1}{a_0} + ip\right)}p^2 + \cdots\right]. \quad (23)$$

Matching the above equation to the LO and NLO terms, $\mathcal{T}_{\rm LO}$ and $\mathcal{T}_{\rm NLO}$, from Eq. (21), as illustrated in Fig. 1, one can derive the relations among the scattering length a_0, effective range r_0, and low-energy couplings C_0 and C_2 as [72,73,79,80]

$$C_0 = \frac{2\pi}{\mu}\frac{1}{\frac{1}{a_0} - \alpha\Lambda}, \quad (24)$$

$$C_2 = \frac{2\pi}{\mu}\frac{1}{\left(\frac{1}{a_0} - \alpha\Lambda\right)^2}\frac{r_0}{2}, \quad (25)$$

where α can be determined with different regulators and renormalization schemes [47]. For the Gaussian form factor we used here, $\alpha\Lambda = \frac{2\pi}{\mu}G(0,\Lambda) \sim 0.4\Lambda$.

IV. POWER COUNTING ANALYSIS

Two power counting schemes—the Weinberg power counting and the KSW (Kaplan, Savage, and Wise) power counting—can both be applied to the above low-energy couplings C_0 and C_2 to ensure that the LO and NLO terms of the amplitude $\mathcal{T}$ are matched to the resummation diagrams depicted in Fig. 1 [81].

Considering a given effective field theory for a particular system, the effective Lagrangian density can be expressed

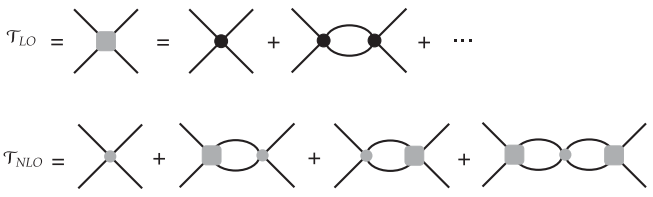

FIG. 1. The s-wave amplitudes of LO and NLO terms from the contact interactions, where black and gray solid circles denote the C_0 and C_2 terms.

in the following form, based on the operator product expansion (OPE)

$$\mathcal{L}_{\text{eff}} = \sum_n C_n \mathcal{O}_n, \tag{26}$$

where $\mathcal{O}_n$ are the operators that satisfy the symmetry requirements for constructing the EFT, and C_n stands for the corresponding Wilsonian coefficient. In this EFT, employing the Wilsonian cutoff Λ, the naive dimensional analysis (NDA) dictates a condition for naturalness, suggesting that the dimensionless parameters in OPE should be of $\mathcal{O}(1)$. Consequently, the different Wilsonian coefficients C_i and C_j associated with the operators $\mathcal{O}_i$ and $\mathcal{O}_j$ are related

$$\frac{C_i}{C_j} \sim \frac{\Lambda^{d_j}}{\Lambda^{d_i}}, \tag{27}$$

where d_i and d_j are the mass dimensions of the operators $\mathcal{O}_i$ and $\mathcal{O}_j$. This relation indicates that for the operators $\mathcal{O}_n$ with higher mass dimensions, the corresponding Wilsonian coefficients C_n will be suppressed compared to those with lower mass dimensions. The above conclusion regarding Wilsonian coefficients from NDA is consistent with Weinberg's power counting used for the contact EFT in Eq. (16), describing the $\bar{D}^{(*)}\Sigma_c^{(*)}$ interactions, where the ratio between C_2 and C_0 is derived as

$$\frac{C_2}{C_0} \sim \Lambda^{-2}, \tag{28}$$

since C_2 is of $\mathcal{O}(p^2)$ while C_0 is of $\mathcal{O}(p^0)$.

Introducing the scheme of *power divergence subtraction* (PDS) in dimensional regularization, Kaplan *et al.* [72,73] suggest that for the large scattering length situation, the couplings C_0 and C_2 in Eqs. (24) and (25) will scale as

$$\frac{C_2}{C_0} \sim \frac{1}{\Lambda(\alpha\Lambda)}. \tag{29}$$

It is clear that with $\alpha\Lambda \to \Lambda$, Weinberg's power counting in Eq. (28) will be recovered, while the choice of $\alpha\Lambda \to p$ leads to the KSW counting [81].

V. MATCHING THE EFFECTIVE RANGE WITH THE NLO CONTACT POTENTIAL

To determine the effective range r_0, it is necessary to include the NLO momentum-related term of the contact potential, as given in Eqs. (18)–(20), to describe the $P_c(4312)$, $P_c(4440)$, and $P_c(4457)$ pentaquarks. With the on-shell approximation, the $\bar{D}^{(*)}\Sigma_c$ potentials can be expressed as

$$V(\bar{D}\Sigma_c) = C_a + D_a p_{cm1}^2, \tag{30}$$

$$V\left(\bar{D}^*\Sigma_c, \frac{1^-}{2}\right) = C_a - \frac{4}{3}C_b + (D_a - D_b)p_{cm2}^2, \tag{31}$$

$$V\left(\bar{D}^*\Sigma_c, \frac{3^-}{2}\right) = C_a + \frac{2}{3}C_b + \left(D_a + \frac{D_b}{2}\right)p_{cm2}^2 \tag{32}$$

where p_{cm1} and p_{cm2} are the center-of-mass momenta for $\bar{D}\Sigma_c$ and $\bar{D}^*\Sigma_c$, respectively, given by

$$p_{cm} = \frac{\sqrt{[s-(m_1+m_2)^2][s-(m_1-m_2)^2]}}{2\sqrt{s}}. \tag{33}$$

Here, $\sqrt{s}$ represents the center-of-mass energy, m_1 and m_2 denote the masses of $\bar{D}^{(*)}$ and Σ_c. However, because there are only three experimental masses, it is impossible to predict the effective ranges from the potential given in Eqs. (30)–(32) with four low-energy couplings, i.e., C_a, C_b, D_a, and D_b. Therefore, we propose three schemes to address this issue:

(I) In scheme I, we neglect the spin-spin interaction term at $\mathcal{O}(p_{cm}^2)$ of the potential in Eqs. (30)–(32), namely, setting $D_b = 0$. This approach is reasonable because the difference in the C_2 term is of the next-to-leading order (NLO) and should contribute less than other terms [82].

(II) In scheme II, including the $P_c(4380)$ discovered by LHCb in 2015,[1] we now have four masses of the $P_c(4312)$, $P_c(4440)$, $P_c(4457)$, and $P_c(4380)$ states, thus the four low-energy couplings could be determined, allowing us to derive the effective range r_0 for the $\bar{D}^{(*)}\Sigma_c^{(*)}$ molecules. In this way, we can check whether including the $P_c(4380)$ mass predicts the expected large $a_0 \gg 1/m_{\text{ex}}$ and natural $r_0 \sim 1/m_{\text{ex}}$, as suggested by Eqs. (8) and (9) for the conjected molecular picture of the pentaquarks, thereby providing insight into the existence of the $P_c(4380)$ state.

(III) In scheme III, the suppression of the NLO low-energy couplings from the power counting can be utilized to estimate the D_b term, allowing to fix four couplings with three inputs.

According to Eqs. (30)–(32) and considering that the NLO D_b term might be suppressed around Λ^2 compared to the LO couplings [see Eqs. (28) and (29)], we can vary D_b within a range of

$$D_b \sim N \times \frac{1}{\Lambda^2} \times [-C, C], \tag{34}$$

[1]Note that the broad $P_c(4380)$ with a large decay width has not been confirmed in later LHCb experiments as mentioned in the Introduction [83]. Nevertheless, some studies have reproduced the $P_c(4380)$ mass through different methods, such as the production rates analysis of pentaquarks [41] and mass spectrum prediction of the seven P_c multiplets [40].

where $N \sim 10$ is the magnitude chosen to ensure that the D_b contribution can be fully considered, and $C \sim 3$ fm^2 is the value of the LO couplings C_0 of C_a, $C_a - \frac{4}{3}C_b$, and $C_a + \frac{2}{3}C_b$ for $P_c(4312)$, $P_c(4440)$, and $P_c(4457)$.

Given that D_b has been determined within the above-specified range, the other three couplings of C_a, C_b, and D_a could be fixed by solving the Lippmann-Schwinger equation for the $\bar{D}^{(*)}\Sigma_c$ systems to reproduce the $P_c(4312)$, $P_c(4440)$, and $P_c(4457)$ masses.

VI. NUMERICAL RESULTS

As in Ref. [40], we are going to distinguish two scenarios: scenario A corresponds to $P_c(4440)$ having $J^P = \frac{1}{2}^-$ and $P_c(4457)$ having $J^P = \frac{3}{2}^-$, and scenario B represents the alternative assignment.

By checking whether the results for scenario A or B can match the pure molecular picture of large, unnatural scattering length $a_0 \gg 1/m_{\rm ex}$ and natural effective range $r_0 \sim 1/m_{\rm ex}$ as suggested by Eqs. (8) and (9), one hopes to identify the spins of $P_c(4440)$ and $P_c(4457)$. In addition to a_0 and r_0, another parameter R can be defined as below for comparison

$$R = \Lambda^2 \frac{C_2}{C_0}, \tag{35}$$

where the C_2 is the sum of D_a and D_b, and C_0 is the sum of C_a and C_b. The natural value for this $|R|$, calculated from the contact effective field theory we constructed above, is expected to be around $R_{\rm natu} = 1/\alpha \simeq 2.5$ from the power counting given in Eq. (29).

A. Results for scheme I

First, we show the predictions of Scheme I where the D_b coupling, representing the NLO spin-spin interaction term, is simply neglected in Eqs. (30)–(32). Taking the masses of the $P_c(4312)$, $P_c(4440)$, and $P_c(4457)$ states as inputs, the resulting scattering length a_0 and effective range r_0 for these three pentaquarks are summarized in Table I.

The effective range r_0 of $P_c(4440)$ and $P_c(4457)$ are positive in scenario B but negative in scenario A. This result indicates that, in the molecule picture, it is more natural to identify $P_c(4440)$ as the $J^P = \frac{3}{2}^-$ $\bar{D}^*\Sigma_c$ molecule and $P_c(4457)$ as the $J^P = \frac{1}{2}^-$ one. Additionally, the positive effective ranges derived for scenario B fall within the range of $[0.4, 0.75]$ fm, which is indeed of the order of $\mathcal{O}(1/m_{\rm ex})$, assuming the mass $m_{\rm ex}$ of the exchanged meson mediating the $\bar{D}^{(*)}\Sigma_c$ interaction is approximately 500 MeV. This is close to the masses of mesons such as σ, ρ, ω, which are often considered in the context of the one-boson exchange model for the $\bar{D}^{(*)}\Sigma_c$ molecules. These results for r_0 are consistent with the conclusion from the Weinberg compositeness criterion in Eq. (9) that for pure molecular states with $Z = 0$, r_0 should be positive and of the order of $\mathcal{O}(1/m_{\rm ex})$.

Furthermore, the large scattering length $a_0 \gg 1/m_{\rm ex}$ predicted for scenario B is also around $1/\gamma$ as expected from Eq. (8), where $\gamma = \sqrt{2\mu E_B} \sim 100$–$200$ MeV are the binding momenta of $P_c(4312)$, $P_c(4440)$, and $P_c(4457)$ in the $\bar{D}^{(*)}\Sigma_c$ molecular picture.

B. Results for scheme II

In Scheme 2, the $P_c(4380)$ is considered as an additional input alongside $P_c(4312)$, $P_c(4440)$, and $P_c(4457)$. With the masses of these four pentaquark states, the four couplings appearing in Eqs. (30)–(32) can now all be fixed. The effective ranges for $P_c(4380)$, $P_c(4312)$, $P_c(4440)$, and $P_c(4457)$ are all positive for either scenario A or B, suggesting that both are consistent with the molecular picture. However, among the predicted positive r_0 for these four pentaquarks, there are always three with a magnitude larger than the natural value of order $\mathcal{O}(1/m_{\rm ex})$, which does not fit well with the molecular picture.

The ratios R in Eq. (35) for the four P_c states, listed in Table II, are often 10-30 times greater than Λ^{-2} for both scenarios A and B, which deviate significantly from the expectation of $1/\alpha \simeq 2.5$ as required by the power counting in Eqs. (29) and (35).

These abnormal a_0, r_0, and R obtained for both spin assignments suggest that $P_c(4380)$ might not be considered

TABLE I. The scattering length a_0, effective range r_0, and parameter $|R|$ for $P_c(4312)$, $P_c(4440)$, and $P_c(4457)$ obtained in scheme I, where the D_b term has been neglected and two cutoffs of 0.5 and 1 GeV are used for Λ. The $P_c(4312)$, $P_c(4440)$, and $P_c(4457)$ states are referred to P_{c1}, P_{c2}, and P_{c3}, respectively.

		a_0(fm)			r_0(fm)			$\lvert R\rvert$		
Scenario	Λ(GeV)	P_{c1}	P_{c2}	P_{c3}	P_{c1}	P_{c2}	P_{c3}	P_{c1}	P_{c2}	P_{c3}
A	0.5	2.09	1.58	2.57	−0.04	−0.02	−0.06	0.3	0.2	0.3
	1	1.42	−0.34	−0.07	−0.54	−0.31	−0.72	5.3	4.1	6.2
B	0.5	2.88	2.45	3.40	0.61	0.53	0.75	3.0	3.4	2.8
	1	2.24	1.74	2.75	0.50	0.44	0.58	4.1	4.5	4.0

TABLE II. The scattering length a_0, effective range r_0, and parameter $|R|$ for $P_c(4312)$, $P_c(4380)$, $P_c(4440)$, and $P_c(4457)$ obtained in scheme II with two cutoffs of 0.5 and 1 GeV are used for Λ. The $P_c(4312)$, $P_c(4440)$, $P_c(4457)$, and $P_c(4380)$ are referred to as P_{c1}, P_{c2}, P_{c3}, and P_{c4}, respectively.

		a_0(fm)				r_0(fm)				$\|R\|$			
Scenario	Λ(GeV)	P_{c1}	P_{c2}	P_{c3}	P_{c4}	P_{c1}	P_{c2}	P_{c3}	P_{c4}	P_{c1}	P_{c2}	P_{c3}	P_{c4}
A	0.5	5.03	2.88	6.37	4.81	1.68	0.75	2.28	1.66	6.7	3.6	8.6	6.7
	1	5.01	2.07	7.00	4.55	1.87	0.65	2.62	1.85	13.2	5.5	17.9	13.2
B	0.5	5.01	3.29	32.82	4.81	1.68	0.93	4.10	1.66	6.7	13.5	4.2	6.7
	1	5.01	2.54	−27.30	4.55	1.87	0.89	4.62	1.85	13.2	28.9	7.0	13.2

a molecular state together with $P_c(4312)$, $P_c(4440)$, and $P_c(4457)$. The $P_c(4380)$ may be excluded as an HQSS molecular partner of P_c states. However, we will demonstrate below that the classification of $P_c(4380)$ as the HQSS partner is sensitive to its mass, where the broad $P_c(4380)$ discovered in 2015 cannot yet be ruled out because its mass, predicted from scenario B to be around ∼4376 MeV, is within the experimental uncertainty range for the $P_c(4380)$ mass.

C. Results for scheme III

Introducing the variation in Eq. (34) based on the EFT power counting, the D_b coupling can vary within a reasonable range. For each D_b value within this range, the other three low-energy coupling of C_a, C_b, and D_a can be fixed by identifying the $\mathcal{T}$ poles in Eq. (21) as $P_c(4312)$, $P_c(4440)$, and $P_c(4457)$ for $\bar{D}^{(*)}\Sigma_c$ molecules.

In Fig. 2, we present the variations of R and r_0 of $P_c(4312)$, $P_c(4440)$, and $P_c(4457)$ as functions of D_b. For scenario A [see Figs. 2(a) and 2(b)], for both cutoffs of $\Lambda = 0.5$ GeV and $\Lambda = 1$ GeV, the effective range r_0 cannot simultaneously have a natural positive value around $\mathcal{O}(1/m_{\rm ex}) \sim 0.5$ fm for $P_c(4312)$, $P_c(4440)$, and $P_c(4457)$. In addition, the ratio R for these pentaquarks exceeds the natural range of $\mathcal{O}(1/\alpha) \simeq 2.5$ for r_0 around $\mathcal{O}(1/m_{\rm ex})$ (shaded area with $0 < r_0 < 1$ fm in Fig. 2).

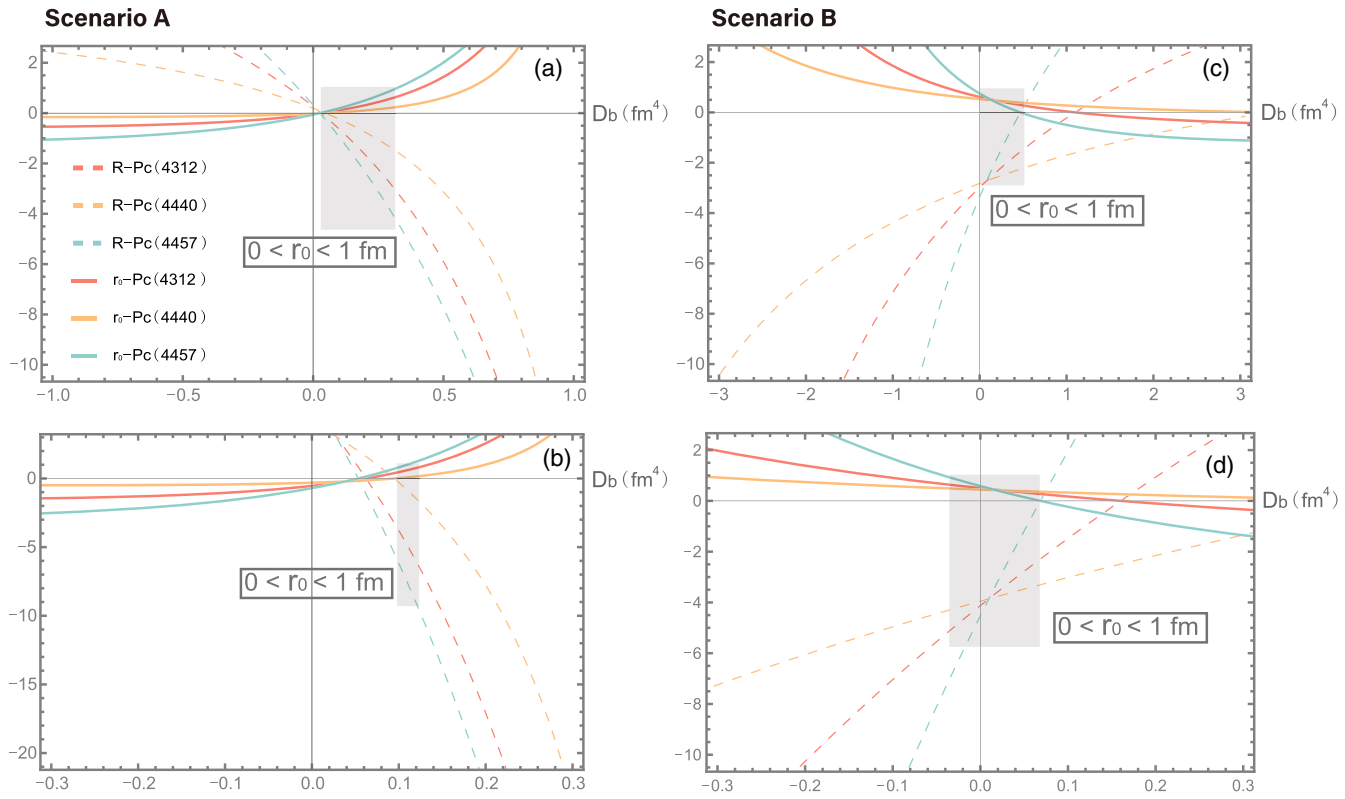

FIG. 2. The ratio R and effective range r_0 of $P_c(4312)$, $P_c(4440)$, and $P_c(4457)$ obtained for scheme III. Panels (a) and (b) show the R and r_0 results for scenario A with two cutoffs of $\Lambda = 0.5$ GeV and $\Lambda = 1$ GeV, while panels (c) and (d) show the R and r_0 results for scenario B with two cutoffs of $\Lambda = 0.5$ GeV and $\Lambda = 1$ GeV.

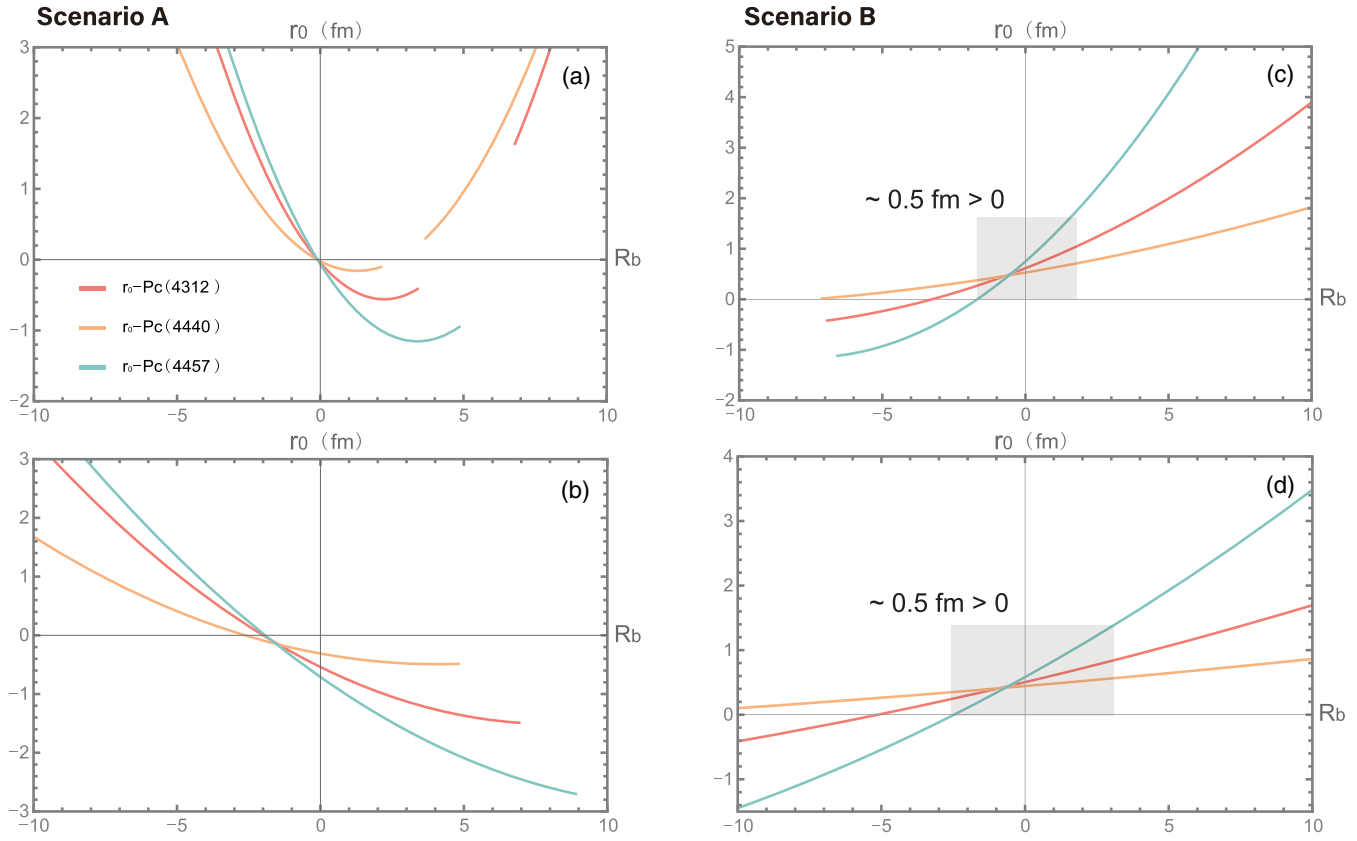

FIG. 3. The variation of the effective range r_0 with the ratio R_b for $P_c(4312)$, $P_c(4440)$, and $P_c(4457)$ obtained for scheme III. Panels (a) and (b) show the r_0 results for scenario A with two cutoffs of $\Lambda = 0.5$ GeV and $\Lambda = 1$ GeV, while panels (c) and (d) denote the r_0 results for scenario B with two cutoffs of $\Lambda = 0.5$ GeV and $\Lambda = 1$ GeV.

However, for scenario B [see Figs. 2(c) and 2(d)], the same positive effective range r_0 around $\mathcal{O}(1/m_{\rm ex}) \sim 0.5$ fm for $P_c(4312)$, $P_c(4440)$, and $P_c(4457)$ can be obtained for a natural value of $|R| \sim 1$–3. This result corroborates again the conclusion obtained for Scheme I, indicating that in the HQSS framework, $P_c(4440)$ should have spin-parity $J^P = \frac{3}{2}^-$ and $P_c(4457)$ spin-parity $J^P = \frac{1}{2}^-$.

We also study the relation between the predicted effective range r_0 and the value of $R_b = \Lambda^2 \frac{D_b}{C_0}$ to check further the naturalness of the contact EFT we employed. Only the NLO D_b coupling is chosen to study the power counting. C_0 corresponds to C_a, $C_a - \frac{4}{3}C_b$, and $C_a + \frac{2}{3}C_b$ for the three P_c states, respectively. Figure 3 shows that the effective ranges r_0 of $P_c(4312)$, $P_c(4440)$, and $P_c(4457)$ in scenario A are negative for R_b around the natural range of $[-3, 3]$. However, in scenario B, while R_b varies within $[-3, 3]$, the effective ranges r_0 for $P_c(4312)$, $P_c(4440)$, and $P_c(4457)$ are of natural positive values of $\mathcal{O}(1/m_{\rm ex}) \sim 0.5$ fm, consistent with Eq. (9). These results are also consistent with the conclusion drawn from Fig. 2, indicating that it is more natural to consider $P_c(4440)$ as the $J^P = \frac{3}{2}^-$ and $P_c(4457)$ as the $J^P = \frac{1}{2}^-$ $\bar{D}^*\Sigma_c$ states if $P_c(4312)$, $P_c(4440)$, and $P_c(4457)$ are $\bar{D}^{(*)}\Sigma_c$ heavy-quark symmetry partners in the molecular picture.

From the condition where positive $r_0 \sim \mathcal{O}(1/m_{\rm ex})$ of the three P_c pentaquarks simultaneously emerge together with the natural $R \sim 2.5$ in scenario B, the $D_b \sim 0.15$ fm^4 and $\sim$0.03 fm^4 can be determined for $\Lambda = 0.5$ GeV and

TABLE III. With $D_b \sim 0.15$ fm^4 and $\sim$0.03 fm^4 for $\Lambda = 0.5$ GeV and $\Lambda = 1$ GeV from scenario B, the mass of $\bar{D}\Sigma_c^*$, the scattering length a_0, the effective range r_0, and the parameter R for $P_c(4312)$, $P_c(4380)$, $P_c(4440)$, and $P_c(4457)$ are predicted.

		a_0(fm)				r_0(fm)				$\lvert R\rvert$			
Λ(GeV)	$m_{\bar{D}\Sigma_c^*}$(MeV)	P_{c1}	P_{c2}	P_{c3}	P_{c4}	P_{c1}	P_{c2}	P_{c3}	P_{c4}	P_{c1}	P_{c2}	P_{c3}	P_{c4}
0.5	4375.84	2.73	2.37	3.08	2.67	0.50	0.48	0.46	0.49	2.50	2.63	2.19	2.50
1	4375.6	2.13	1.69	2.52	2.06	0.40	0.41	0.31	0.39	3.31	3.67	2.49	3.31

$\Lambda = 1$ GeV, respectively [see Figs. 2(c) and 2(d)]. The above D_b couplings can predict whether the broad $P_c(4380)$ state could be regarded as a $\bar{D}\Sigma_c^*$ molecule. From the results shown in Table III, the $P_c(4380)$ mass is predicted as follows

$$m_{P_c(4380)} = 4375.84 \text{ MeV}(\Lambda = 0.5 \text{ GeV}), \quad (36)$$

$$m_{P_c(4380)} = 4375.6 \text{ MeV}(\Lambda = 1 \text{ GeV}). \quad (37)$$

These values are approximately 4 MeV below the central mass value of the $P_c(4380)$ state as observed in 2015, but they remain comfortably within the experimental uncertainties [6]. Therefore, the broad $P_c(4380)$ cannot yet be excluded as the HQSS molecular partner of $P_c(4312)$, $P_c(4440)$, and $P_c(4457)$; meanwhile the predicted mass of $P_c(4380)$ is constrained to ~4376 MeV based on the naturalness of the power counting of the contact effective field theory.

VII. DISCUSSION AND CONCLUSION

This study investigated the effective ranges of the recently discovered $P_c(4312)$, $P_c(4440)$, and $P_c(4457)$ states in the molecular picture and the contact effective field theory framework. The Weinberg compositeness criterion indicates for a pure hadronic molecular state, the effective range r_0 should be positive and of the order of $\mathcal{O}(1/m_{\text{ex}})$, while the scattering length is unnaturally large, i.e., $a_0 \gg \mathcal{O}(1/m_{\text{ex}})$.

Taking into account two alternative spin assignments for $P_c(4440)$ and $P_c(4457)$, we proposed three schemes for the NLO contact potentials. This allowed us to determine the scattering length a_0, effective range r_0, and the parameter R, where R is quantified through a naturalness criterion dictated by the power counting, for the $P_c(4312)$, $P_c(4440)$, and $P_c(4457)$ pentaquarks.

We showed that only scenario B can accommodate simultaneously a positive effective range $r_0 \sim \mathcal{O}(1/m_{\text{ex}})$, a large scattering length $a_0 \gg \mathcal{O}(1/m_{\text{ex}})$, and a natural $R \sim 2.5$. As a result, it seems to be more natural to assign $J^P = \frac{3}{2}^-$ to $P_c(4440)$ and $J^P = \frac{1}{2}^-$ to $P_c(4457)$ in the molecular $\bar{D}^*\Sigma_c$ picture. This conclusion agrees with Refs. [31,41,45,84,85] and indicates that within the molecular states composed of the same components, the pentaquarks with higher spin prefer a lower mass. This is consistent with scenario B of Ref. [40].

It should be noted that our study is performed in single channel. Coupled-channel effects, such as $\bar{D}\Lambda_{c1}(2595)$ [86,87], might alter the aforementioned conclusion. This is because the threshold for $\bar{D}\Lambda_{c1}(2595)$ is close to $P_c(4440)$ and $P_c(4457)$, and it may couple with $\bar{D}^*\Sigma_c$. However, limited by the available mass inputs, determining the potential of $\bar{D}\Lambda_{c1}(2595) - \bar{D}\Lambda_{c1}(2595)$ and crossed-channel $\bar{D}\Lambda_{c1}(2595) - \bar{D}^*\Sigma_c$ is challenging. Consequently, studying the effective range within coupled-channel are beyond the scope of our current work. Additionally, we assumed $Z = 0$ to obtain $r_0 > 0$. Therefore, if $P_c(4312)$, $P_c(4440)$, and $P_c(4457)$ contain a significant compact component, the above conclusion of positive r_0 might change. Nevertheless, the range of r_0 being estimated as $|r_0| \sim \mathcal{O}(1/m_{\text{ex}})$ should still be satisfied for dominantly molecular states.

Moreover, since the LHCb data of 2019 can be fitted equally well by models that either include or exclude the Breit-Wigner contribution from $P_c(4380)$, the potential role of $P_c(4380)$ as a HQSS molecule, akin to $P_c(4312)$, $P_c(4440)$, and $P_c(4457)$, remains uncertain. Our results for scheme II and III suggest that if the $P_c(4380)$ is to be regarded as the HQSS molecular partner of $\bar{D}\Sigma_c^*$ alongside $P_c(4312)$, $P_c(4440)$, and $P_c(4457)$, its mass should be constrained to around 4376 MeV based on the naturalness argument from the power counting, which resides roughly 4 MeV below the experimental central mass of $P_c(4380)$.

These findings about discriminating the spins of P_c states and constraining the hidden-charm pentaquark predictions are relevant for future experimental investigations and further theoretical studies on the inner structure of pentaquarks.

ACKNOWLEDGMENTS

We would like to thank Mao-Jun Yan, Jun-Xu Lu, Eulogio Oset and Manuel Pavon Valderrama for the helpful discussions. This work is partly supported by the National Key R&D Program of China under Grant No. 2023YFA1606703, the Postdoctoral Fellowship Program of CPSF under Grant No. GZC20241765, the Postdoctoral Fellowship Program of Gansu Province, and by the National Natural Science Foundation of China under Grants No. 12075288, No. 12435007, and No. 12361141819. It is also supported by the Youth Innovation Promotion Association CAS.

DATA AVAILABILITY

The data that support the findings of this article are openly available [71].

[1] M. Gell-Mann, Phys. Lett. **8**, 214 (1964).
[2] G. Zweig (1964), 10.17181/CERN-TH-401.
[3] N. Brambilla *et al.*, Eur. Phys. J. C **71**, 1534 (2011).
[4] A. Esposito, A. Pilloni, and A. D. Polosa, Phys. Rep. **668**, 1 (2017).
[5] A. Ali, J. S. Lange, and S. Stone, Prog. Part. Nucl. Phys. **97**, 123 (2017).
[6] R. Aaij *et al.* (LHCb Collaboration), Phys. Rev. Lett. **115**, 072001 (2015).
[7] R. Aaij *et al.* (LHCb Collaboration), Phys. Rev. Lett. **122**, 222001 (2019).
[8] H.-X. Chen, W. Chen, X. Liu, and S.-L. Zhu, Phys. Rep. **639**, 1 (2016).
[9] F.-K. Guo, C. Hanhart, U.-G. Meißner, Q. Wang, Q. Zhao, and B.-S. Zou, Rev. Mod. Phys. **90**, 015004 (2018); **94**, 029901(E) (2022).
[10] C. Fernández-Ramírez, A. Pilloni, M. Albaladejo, A. Jackura, V. Mathieu, M. Mikhasenko, J. A. Silva-Castro, and A. P. Szczepaniak (JPAC Collaboration), Phys. Rev. Lett. **123**, 092001 (2019).
[11] Y.-R. Liu, H.-X. Chen, W. Chen, X. Liu, and S.-L. Zhu, Prog. Part. Nucl. Phys. **107**, 237 (2019).
[12] F.-K. Guo, H.-J. Jing, U.-G. Meißner, and S. Sakai, Phys. Rev. D **99**, 091501 (2019).
[13] C. W. Xiao, J. Nieves, and E. Oset, Phys. Rev. D **100**, 014021 (2019).
[14] F.-L. Wang, R. Chen, Z.-W. Liu, and X. Liu, Phys. Rev. C **101**, 025201 (2020).
[15] L. Meng, B. Wang, G.-J. Wang, and S.-L. Zhu, Phys. Rev. D **100**, 014031 (2019).
[16] J.-J. Wu, T. S. H. Lee, and B.-S. Zou, Phys. Rev. C **100**, 035206 (2019).
[17] M. B. Voloshin, Phys. Rev. D **100**, 034020 (2019).
[18] T. J. Burns and E. S. Swanson, Phys. Rev. D **100**, 114033 (2019).
[19] J.-J. Wu, R. Molina, E. Oset, and B. S. Zou, Phys. Rev. Lett. **105**, 232001 (2010).
[20] W. L. Wang, F. Huang, Z. Y. Zhang, and B. S. Zou, Phys. Rev. C **84**, 015203 (2011).
[21] Z.-C. Yang, Z.-F. Sun, J. He, X. Liu, and S.-L. Zhu, Chin. Phys. C **36**, 6 (2012).
[22] S. G. Yuan, K. W. Wei, J. He, H. S. Xu, and B. S. Zou, Eur. Phys. J. A **48**, 61 (2012).
[23] J.-J. Wu, T. S. H. Lee, and B. S. Zou, Phys. Rev. C **85**, 044002 (2012).
[24] C. W. Xiao, J. Nieves, and E. Oset, Phys. Rev. D **88**, 056012 (2013).
[25] T. Uchino, W.-H. Liang, and E. Oset, Eur. Phys. J. A **52**, 43 (2016).
[26] M. Karliner and J. L. Rosner, Phys. Rev. Lett. **115**, 122001 (2015).
[27] M.-Z. Liu, F.-Z. Peng, M. Sánchez Sánchez, and M. P. Valderrama, Phys. Rev. D **98**, 114030 (2018).
[28] Z.-H. Guo and J. A. Oller, Phys. Lett. B **793**, 144 (2019).
[29] S. Sakai, H.-J. Jing, and F.-K. Guo, Phys. Rev. D **100**, 074007 (2019).
[30] F.-Z. Peng, J.-X. Lu, M. Sánchez Sánchez, M.-J. Yan, and M. Pavon Valderrama, Phys. Rev. D **103**, 014023 (2021).
[31] M.-L. Du, V. Baru, F.-K. Guo, C. Hanhart, U.-G. Meißner, J. A. Oller, and Q. Wang, J. High Energy Phys. 08 (2021) 157.
[32] F.-Z. Peng, M.-J. Yan, M. S. Sánchez, and M. Pavon Valderrama, Phys. Lett. B **846**, 138207 (2023).
[33] M.-Z. Liu, Y.-W. Pan, Z.-W. Liu, T.-W. Wu, J.-X. Lu, and L.-S. Geng, Phys. Rep. **1108**, 1 (2025).
[34] R. Zhu, X. Liu, H. Huang, and C.-F. Qiao, Phys. Lett. B **797**, 134869 (2019).
[35] A. Ali and A. Y. Parkhomenko, Phys. Lett. B **793**, 365 (2019).
[36] M. I. Eides, V. Y. Petrov, and M. V. Polyakov, Mod. Phys. Lett. A **35**, 2050151 (2020).
[37] J. F. Giron, R. F. Lebed, and C. T. Peterson, J. High Energy Phys. 05 (2019) 061.
[38] S.-Q. Kuang, L.-Y. Dai, X.-W. Kang, and D.-L. Yao, Eur. Phys. J. C **80**, 433 (2020).
[39] H. Garcilazo and A. Valcarce, Phys. Rev. D **105**, 114016 (2022).
[40] M.-Z. Liu, Y.-W. Pan, F.-Z. Peng, M. Sánchez Sánchez, L.-S. Geng, A. Hosaka, and M. Pavon Valderrama, Phys. Rev. Lett. **122**, 242001 (2019).
[41] M.-L. Du, V. Baru, F.-K. Guo, C. Hanhart, U.-G. Meißner, J. A. Oller, and Q. Wang, Phys. Rev. Lett. **124**, 072001 (2020).
[42] M. Pavon Valderrama, Phys. Rev. D **100**, 094028 (2019).
[43] R. Chen, Z.-F. Sun, X. Liu, and S.-L. Zhu, Phys. Rev. D **100**, 011502 (2019).
[44] Z.-W. Liu, J.-X. Lu, M.-Z. Liu, and L.-S. Geng, Phys. Rev. D **108**, L031503 (2023).
[45] M.-Z. Liu, T.-W. Wu, M. Sánchez Sánchez, M. P. Valderrama, L.-S. Geng, and J.-J. Xie, Phys. Rev. D **103**, 054004 (2021).
[46] Z. Zhang, J. Liu, J. Hu, Q. Wang, and U.-G. Meißner, Sci. Bull. **68**, 981 (2023).
[47] H. W. Hammer, S. König, and U. van Kolck, Rev. Mod. Phys. **92**, 025004 (2020).
[48] L. Contessi, M. Pavon Valderrama, and U. van Kolck, Phys. Lett. B **856**, 138903 (2024).
[49] S. Weinberg, Phys. Rev. **130**, 776 (1963).
[50] S. Weinberg, Phys. Rev. **137**, B672 (1965).
[51] U. van Kolck, Symmetry **14**, 1884 (2022).
[52] V. Baru, X.-K. Dong, M.-L. Du, A. Filin, F.-K. Guo, C. Hanhart, A. Nefediev, J. Nieves, and Q. Wang, Phys. Lett. B **833**, 137290 (2022).
[53] T. Hyodo, Int. J. Mod. Phys. A **28**, 1330045 (2013).
[54] T. Hyodo, Phys. Rev. Lett. **111**, 132002 (2013).
[55] J. A. Oller, Ann. Phys. (Amsterdam) **396**, 429 (2018).
[56] I. Matuschek, V. Baru, F.-K. Guo, and C. Hanhart, Eur. Phys. J. A **57**, 101 (2021).
[57] Y. Li, F.-K. Guo, J.-Y. Pang, and J.-J. Wu, Phys. Rev. D **105**, L071502 (2022).
[58] J. Song, L. R. Dai, and E. Oset, Eur. Phys. J. A **58**, 133 (2022).
[59] T. Kinugawa and T. Hyodo, arXiv:2411.12285.
[60] L. D. Landau and E. M. Lifshits, *Quantum Mechanics: Non-Relativistic Theory*, Course of Theoretical Physics, Vol. 3 (Butterworth-Heinemann, Oxford, 1991).
[61] A. Esposito, L. Maiani, A. Pilloni, A. D. Polosa, and V. Riquer, Phys. Rev. D **105**, L031503 (2022).

[62] H. A. Bethe, Phys. Rev. **76**, 38 (1949).
[63] J. J. Sakurai and J. Napolitano, *Modern Quantum Mechanics*, Quantum Physics, Quantum Information and Quantum Computation (Cambridge University Press, Cambridge, England, 2020).
[64] L. Meng, B. Wang, G.-J. Wang, and S.-L. Zhu, Phys. Rep. **1019**, 1 (2023).
[65] Y.-B. Shen, M.-Z. Liu, Z.-W. Liu, and L.-S. Geng, Phys. Rev. D **111**, 034001 (2025).
[66] M.-J. Yan, F.-Z. Peng, and M. Pavon Valderrama, Phys. Rev. D **109**, 014023 (2024).
[67] F.-Z. Peng, M. Sánchez Sánchez, M.-J. Yan, and M. Pavon Valderrama, Phys. Rev. D **105**, 034028 (2022).
[68] F.-Z. Peng, M.-Z. Liu, Y.-W. Pan, M. Sánchez Sánchez, and M. Pavon Valderrama, Nucl. Phys. **B983**, 115936 (2022).
[69] F.-Z. Peng, M.-J. Yan, M. Sánchez Sánchez, and M. P. Valderrama, Eur. Phys. J. C **81**, 666 (2021).
[70] M.-J. Yan, F.-Z. Peng, M. Sánchez Sánchez, and M. Pavon Valderrama, Phys. Rev. D **107**, 074025 (2023).
[71] S. Navas *et al.* (Particle Data Group), Phys. Rev. D **110**, 030001 (2024).
[72] D. B. Kaplan, M. J. Savage, and M. B. Wise, Phys. Lett. B **424**, 390 (1998).
[73] D. B. Kaplan, M. J. Savage, and M. B. Wise, Nucl. Phys. **B534**, 329 (1998).
[74] H. W. Hammer and R. J. Furnstahl, Nucl. Phys. **A678**, 277 (2000).
[75] C. Ordonez, L. Ray, and U. van Kolck, Phys. Rev. C **53**, 2086 (1996).
[76] E. Epelbaum, W. Gloeckle, and U.-G. Meissner, Nucl. Phys. **A637**, 107 (1998).
[77] E. Epelbaum, W. Glockle, and U.-G. Meissner, Nucl. Phys. **A747**, 362 (2005).
[78] J. Haidenbauer, S. Petschauer, N. Kaiser, U. G. Meissner, A. Nogga, and W. Weise, Nucl. Phys. **A915**, 24 (2013).
[79] T. D. Cohen, Phys. Rev. C **55**, 67 (1997).
[80] E. Epelbaum, arXiv:1001.3229.
[81] E. Epelbaum, J. Gegelia, and U.-G. Meißner, Nucl. Phys. **B925**, 161 (2017).
[82] J.-Z. Wu, J.-Y. Pang, and J.-J. Wu, Chin. Phys. Lett. **41**, 091201 (2024).
[83] L. Roca and E. Oset, Eur. Phys. J. C **76**, 591 (2016).
[84] N. Yalikun, Y.-H. Lin, F.-K. Guo, Y. Kamiya, and B.-S. Zou, Phys. Rev. D **104**, 094039 (2021).
[85] Y. Yamaguchi, H. García-Tecocoatzi, A. Giachino, A. Hosaka, E. Santopinto, S. Takeuchi, and M. Takizawa, Phys. Rev. D **101**, 091502 (2020).
[86] L. Geng, J. Lu, and M. P. Valderrama, Phys. Rev. D **97**, 094036 (2018).
[87] T. J. Burns and E. S. Swanson, Phys. Rev. D **106**, 054029 (2022).